

“Apical thinning”: Relations between myocardial wall thickness and apical left ventricular tracer uptake as assessed with positron emission tomography myocardial perfusion imaging

Dominik A. Steffen, MBChB,^a Andreas A. Giannopoulos, MD, PhD,^a Marvin Grossmann, MD,^a Michael Messerli, MD,^a Moritz Schwyzer, MD,^a Christoph Gräni, MD,^a Cathérine Gebhard, MD,^a Aju P. Pazhenkottil, MD,^a Philipp A. Kaufmann, MD,^a and Ronny R. Buechel, MD^a

^a Department of Nuclear Medicine, Cardiac Imaging, University Hospital Zurich, Zurich, Switzerland

Received Mar 16, 2018; accepted Jul 27, 2018
doi:10.1007/s12350-018-1397-2

Background. A reduction in left ventricular apical tracer uptake (apical thinning) is frequently observed in myocardial perfusion imaging (MPI), yet its cause remains a matter of debate, particularly in perfusion emission tomography (PET). This analysis sought to determine whether apical thinning in PET-MPI is attributable to true anatomical thinning of the left ventricular apical myocardium.

Methods and Results. We retrospectively analyzed 57 patients without any history or signs of apical myocardial infarction who underwent rest PET-MPI with 13N-ammonia and contrast-enhanced cardiac computed tomography (CT). Semi-quantitative normalized percent apical 13N-ammonia uptake at rest, myocardial blood flow (MBF), and k2 wash-out rate constants were compared to apical myocardial wall thickness measurements derived from CT and base-to-apex gradients were calculated. Apical thinning was found in 93% of patients and in 74% when analysis of normalized apical tracer uptake was confined to end-systole. No significant correlation was found between apical myocardial thickness and apical tracer uptake ($r = -0.080$, $P = .553$), MBF ($r = -0.211$, $P = .115$), or k2 wash-out rate ($r = -0.023$, $P = .872$), nor between apical myocardial thickness and any gradients. A statistically significant but small difference in apical myocardial thickness was observed in patients with moderately to severely reduced apical tracer uptake vs patients with normal to mildly reduced uptake (4.3 ± 0.7 mm vs 4.7 ± 0.7 mm; $P = .043$).

Conclusions. Apical thinning is a highly prevalent finding during 13N-ammonia PET-MPI that is not solely attributable to true anatomical apical wall thickness or the partial volume effect. Other factors that yet need to be identified seem to have a more prominent impact. (J Nucl Cardiol 2020;27:452–60.)

Key Words: PET • MPI • Hybrid imaging • Image analysis

Electronic supplementary material The online version of this article (<https://doi.org/10.1007/s12350-018-1397-2>) contains supplementary material, which is available to authorized users.

The authors of this article have provided a PowerPoint file, available for download at SpringerLink, which summarises the contents of the paper and is free for re-use at meetings and presentations. Search for the article DOI on SpringerLink.com.

Reprint requests: Ronny R. Buechel, Department of Nuclear Medicine, Cardiac Imaging, University Hospital Zurich, Ramistrasse 100, 8091 Zurich, Switzerland; ronny.buechel@usz.ch
1071-3581/\$34.00

Copyright © 2018 American Society of Nuclear Cardiology.

Abbreviations	
AC	Attenuation correction
CABG	Coronary artery bypass grafting
CT	Computed tomography
ED/ES	End-diastole/end-systole
MBF	Myocardial blood flow
MPI	Myocardial perfusion imaging
PET	Positron emission tomography
RS	Rest perfusion score of segment 17
SPECT	Single photon emission computed tomography

See related editorial, pp. 461–464

INTRODUCTION

Reduced radiotracer uptake and retention in the left ventricular apex frequently occur in myocardial perfusion imaging (MPI) using single photon emission computed tomography (SPECT) and positron emission tomography (PET). This phenomenon commonly referred to as apical thinning and usually considered to be a normal variant^{1,2} has repeatedly raised interest among investigators as it poses a diagnostic challenge in nuclear cardiology.^{3–5} However, as of today the cause for this phenomenon remains to be elucidated, and the scarce data available are solely based on SPECT studies with no data on its prevalence and etiology in PET-MPI. A variety of potential causes have been proposed, including partial volume effects,⁶ physiological inhomogeneities in myocardial radiotracer distribution,⁷ artifacts induced by attenuation correction (AC),^{5,8–12} or time-of-flight (TOF) PET data acquisition.¹³ Alternatively, it may be hypothesized that apical thinning as observed in PET-MPI is attributable to true anatomical thinning, which has been documented in some studies based on either autopsy or cardiac computed tomography (CT).^{14–17} Against this background, we have used hybrid imaging combining contrast-enhanced cardiac CT and PET-MPI with ¹³N-ammonia to assess the relation between apical thinning and true anatomical thinning of the left ventricular myocardial apex.

METHODS

Study Population

We retrospectively screened all patients who had undergone both ¹³N-ammonia PET-MPI and contrast-enhanced cardiac CT at our institution between January 2005 and December 2015 ($n = 187$, Figure 1). Patients in whom the scans were acquired with an interval of > 120 days were excluded, as were patients with suspected or known history of apical myocardial

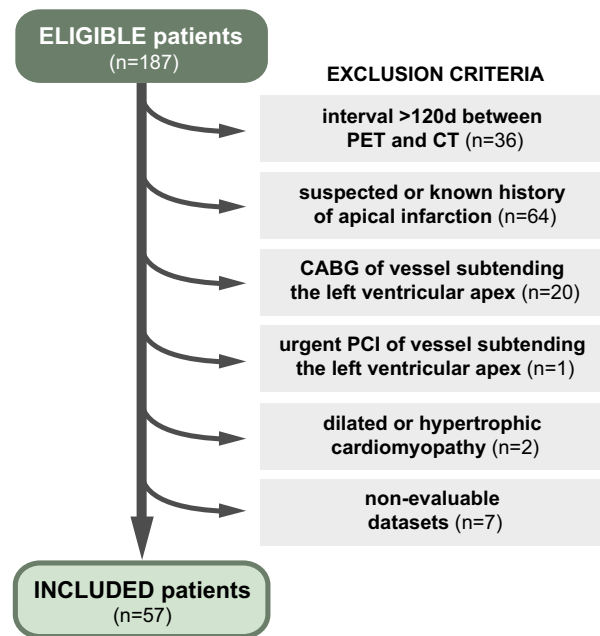


Figure 1. Flowchart illustrating the number of screened, excluded, and included patients. *PCI*, percutaneous coronary intervention; *CABG*, coronary artery bypass grafting.

infarction or with obstructive coronary artery disease in an epicardial coronary artery subtending the apex or the peri-apical region (as assessed by fused hybrid PET/coronary artery CT angiography), patients with a history of coronary artery bypass grafting (CABG) of the vessel subtending the left ventricular apex or those with a history of urgent revascularization of said vessel. Further exclusion criteria were dilated and hypertrophic cardiomyopathies.

PET Image Acquisition

Patients underwent a standard ¹³N-ammonia gated PET-MPI protocol at rest and during adenosine-induced stress (140 µg/min/kg over 7 minutes). Acquisition was performed on either a Discovery RX or Discovery STE PET/CT scanner (both GE Healthcare, Waukesha, WI, USA). ¹³N-ammonia was injected 3 minutes into pharmacologic stress. Rest images were acquired 50 minutes after completion of the stress scan. Mean administered activities were 713 ± 312 MBq for stress and 804 ± 412 MBq for the rest scans. Dynamic 3D ($n = 42$) or 2D ($n = 15$) PET acquisition was started in parallel with the injection and consisted of 9 × 10-s, 6 × 15-s, 3 × 20-s, 2 × 30-s, and 1 × 120-s frames, followed by a static acquisition over 12 minutes. PET data acquired in 3D mode were reconstructed with ordered subset expectation maximization (OSEM; 3 iterations and 16 subsets) while those obtained in 2D

were reconstructed using a filtered back projection (FBP) algorithm with an 8-mm Hanning filter and standard decay scatter sensitivity corrections (voxel size 2.34, 2.34, 3.27). Attenuation maps were derived from low-dose non-contrast enhanced CT scans, and correct alignment with PET datasets was visually verified.

CT Image Acquisition

Contrast-enhanced cardiac CT scans were acquired on a 64-slice (LightSpeed VCT or Discovery CT750 HD) or a 256-slice (Revolution CT, all GE Healthcare, Waukesha, WI, USA) CT scanner. Image acquisition was performed with prospective electrocardiography (ECG) triggering at 75% of the R–R interval. Slice thickness was set to 0.625 mm. Up to 30 mg of metoprolol (Beloc Zok, AstraZeneca, Zug, Switzerland) was administered intravenously to achieve a target heart rate of ≤ 65 bpm. All patients received 2.5 mg isosorbiddinitrate (Isoket, CPS Cito Pharma, Uster, Switzerland) sublingually prior to the scan. Contrast agent (Visipaque 320, GE Healthcare, Opfikon, Switzerland) volume (30 to 105 mL) and flow rate (3.5 to 5 mL/min) were adapted to body mass index.

PET Image Analysis

From the rest scans, normalized semi-quantitative myocardial PET tracer uptake summed across the entire cardiac cycle, end-diastolic (ED) and end-systolic (ES) uptake, quantitative myocardial blood flow (MBF), and the k_2 rate constant (i.e., tracer washout), based on a two-compartment model, were computed using QPET (Version 2015, Cedars-Sinai Medical Center, Los Angeles, CA, USA) and PMOD (Version 3.7, PMOD Technologies, Zurich, Switzerland) and visualized on a 17-segment polar map. Segment 17 was defined as the apex.¹ Apical thinning was defined as a semi-quantitative uptake value of $< 70\%$ in segment 17.¹⁸ Additionally, a segmental rest score (RS) for the apex, as automatically calculated from the QPET software solution¹⁹ and based on a normal database (Figure 2), was recorded according to the 5-point scale ASNC semiquantitative scoring system (0 = no defect, 1 = mildly reduced count density, 2 = moderately reduced, 3 = severely reduced, 4 = absent activity).¹ Patients with normal or only mildly reduced apical counts ($RS < 2$) were compared to individuals with moderate or severe count reduction or absence of counts ($RS \geq 2$). Left ventricular ejection fraction (LVEF) was obtained from gated PET, and heart rate (HR) during PET acquisition was recorded. Additionally, we calculated the base-to-apex gradient for summed tracer uptake, ED uptake, ES uptake, MBF and k_2 expressed

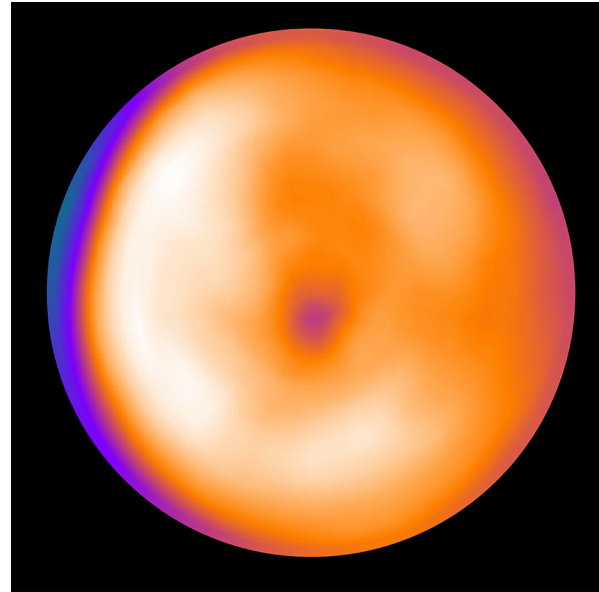


Figure 2. Reference polar map of the normal database used by QPET to calculate segmental rest perfusion scores.

as the ratio between the respective values at the apex and the base as previously described.^{20–23}

CT Image Analysis

Cardiac CT datasets were analyzed on a dedicated workstation (AW 4.7, GE Healthcare). Images were reconstructed as vertical and horizontal long axis views. Window width and level were adjusted for optimal delineation of the myocardial wall. Anterior, inferior, and lateral left ventricular wall thicknesses were defined as the mean of three consecutive measurements at 30 mm intervals, starting at the base (Figure 3). The ventricular septum was excluded from measurement due to poor delineation from the right ventricular cavity. Apical thin point thickness was defined as the mean of the visually identified minimal myocardial wall thickness in both vertical and horizontal reconstructions. Apical wall thickness was averaged from the thin point thickness and adjacent measurements taken at a distance of 10 mm from the thin point in all four directions (Figure 3). Additionally, the measurements of the thin point and the apex were adjusted for interindividual variation in global myocardial wall thickness by expressing them as a fraction of the averaged anterior, inferior, and lateral wall thickness (referred to as “indexed” values). Additionally, we calculated the base-to-apex gradient expressed as the ratio between apical wall thickness and the mean of measurements A2, I2 and L2 (Figure 3).

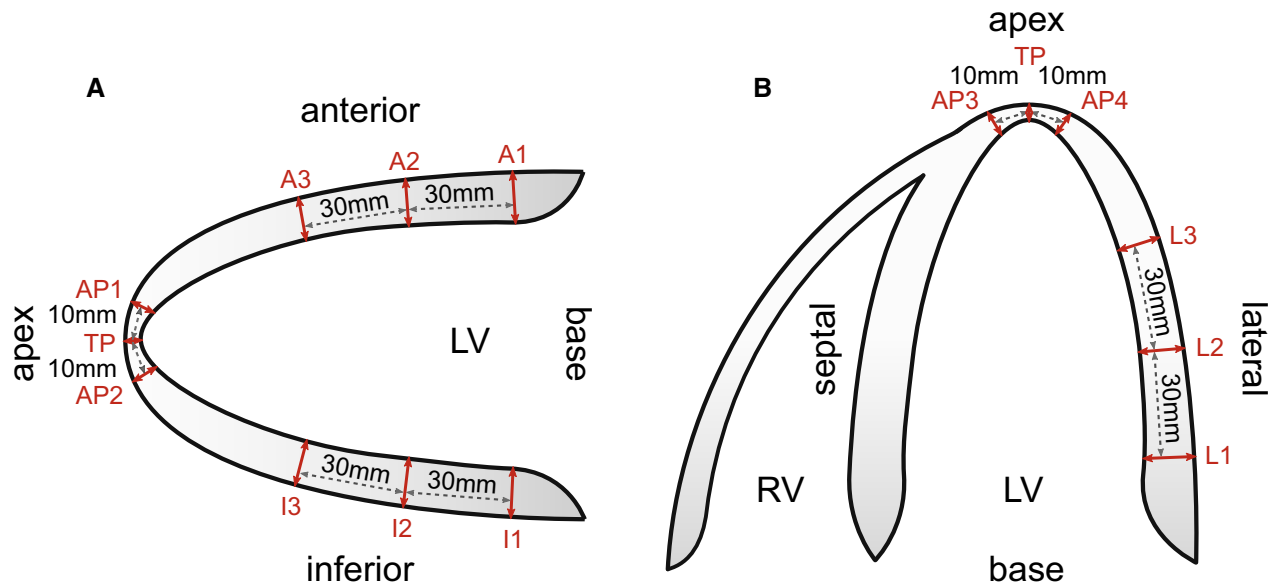


Figure 3. Schematic of left ventricular myocardial wall thickness measurement sites on vertical (A) and horizontal (B) long axis CT reconstructions. TP, thin point; AP1-4, apex measurements; A1-3, anterior wall; I1-3, inferior wall; L1-3, lateral wall.

Statistics

All statistical analyses were performed using IBM SPSS Statistics 25 (IBM Corporation, Armonk, NY, USA). Continuous variables are expressed as mean \pm standard deviation (SD) and paired or unpaired Student's *t*-test was used for comparison. Categorical variables are listed as frequencies (%) and were compared with the Pearson χ^2 test. Pearson correlation coefficients were used to measure the relation between myocardial wall thickness and PET-derived values. A *P*-value of $< .05$ was considered significant.

Ethics

The study was approved by the local ethics committee (BASEC-Nr. 2016-00177) and conforms to the Declaration of Helsinki.

RESULTS

Fifty-seven patients were included in the final analysis (Figure 1). Patient baseline characteristics are given in Table 1.

PET-MPI

Mean semi-quantitative normalized apical tracer uptake was $58.6 \pm 7.1\%$ and 53 patients (93%) had apical thinning (i.e., an apical uptake of $< 70\%$). Mean

rest MBF at the apex was 0.68 ± 0.28 mL/g/min and mean *k*₂ rate constant was 0.29 ± 0.18 /min. When confining analysis of normalized apical tracer uptake to ED, all 57 patients (100%) exhibited apical thinning compared to 43 patients (73.7%) at ES. Furthermore, apical tracer uptake increased significantly from ED to ES ($43.0 \pm 5.9\%$ vs $62.9 \pm 9.2\%$, $P < .001$). When compared to the normal database, perfusion at the apex was deemed normal (RS = 0) in 31.6% of cases ($n = 18$), whereas 22.8% ($n = 13$) were classified as having a mild (RS = 1), and 45.6% ($n = 26$) a moderate uptake reduction (RS = 2). Mean semi-quantitative normalized apical tracer uptake for patients with an apical RS < 2 ($n = 31$) and those with an apical RS ≥ 2 was $62.5 \pm 6.3\%$ and $53.9 \pm 4.8\%$, respectively ($P < .0001$). In patients with an apical RS ≥ 2 , lower apical MBF was measured than in patients with RS < 2 (0.60 ± 0.20 mL/g/min vs 0.75 ± 0.32 mL/g/min; $P = .044$). Apical *k*₂ constants were 0.30 ± 0.22 /min in patients with RS ≥ 2 and 0.29 ± 0.15 /min in patients with RS < 2 ($P = .892$), respectively.

CT Myocardial Thickness Measurements

Myocardial wall thickness measurements are given in Table 2. We observed a minimal but statistically significant difference in apical wall thickness between patients with RS < 2 and RS ≥ 2 (4.7 ± 0.7 mm vs

Table 1. Patient characteristics

Characteristic	All patients (n = 57)	RS < 2 (n = 31)	RS ≥ 2 (n = 26)	P-value*
Male gender, n (%)	41 (71.9%)	22 (71.0%)	19 (73.1%)	.860
Age (years), mean ± SD	64.0 ± 9.8	66.3 ± 9.0	61.2 ± 10.2	.050
BMI (kg/m ²), mean ± SD	28.3 ± 5.9	27.8 ± 6.3	28.9 ± 5.5	.502
LVEF (%), mean ± SD	63.2 ± 12.1	64.5 ± 12.0	61.6 ± 12.1	.364
HR (1/min), mean ± SD	61.5 ± 10.5	62.7 ± 10.8	60.0 ± 10.0	.322

SD, standard deviation; BMI, body mass index; LVEF, left ventricular ejection fraction at rest; HR, heart rate at rest; RS, segment 17 rest score

*P for comparison of RS < 2 vs RS ≥ 2

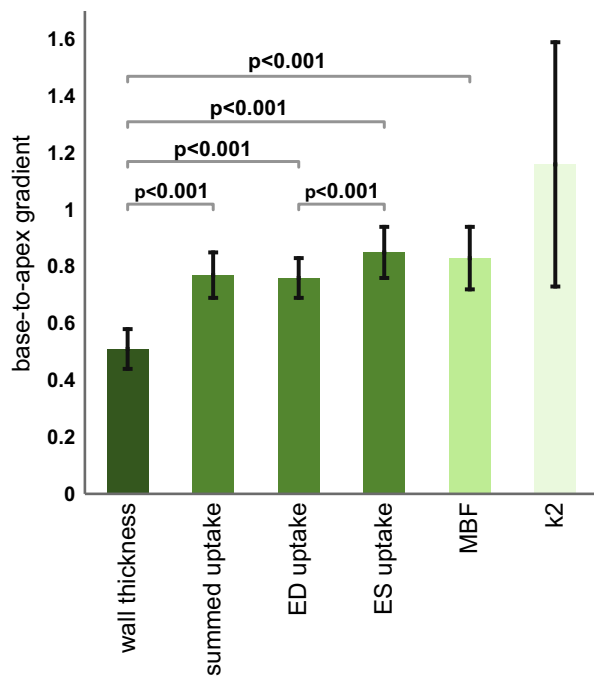


Figure 4. Base-to-apex gradients depicted as mean ± SD (error bars).

4.3 ± 0.7 mm; P = .043), while all other parameters did not differ between the groups.

Base-to-Apex Gradients from PET and CT

All PET-derived values (i.e., end-diastolic, end-systolic, and summed uptake, MBF and k2), as well as CT-derived myocardial wall thickness, showed a significant base-to-apex gradient (Table 3). While tracer uptake, MBF and wall thickness declined from base to apex, k2 rate constants were higher at the apex compared to the base. The inter-individual range for each gradient is depicted in Figure 4. Of note, gradients for summed tracer uptake, ED, and ES uptake as well as MBF were all significantly less inclining than the gradient of myocardial wall thickness. Finally, the gradient for tracer uptake was inclining more at ED than at ES (0.76 ± 0.07 vs 0.85 ± 0.09, P < .001).

Correlation Between PET and CT Findings

No correlation was observed between apical semi-quantitative tracer uptake and the apical thin point

Table 2. Myocardial thickness measurements

Measurement site	All patients (n = 57)	RS < 2 (n = 31)	RS ≥ 2 (n = 26)	P-value*
Anterior wall (mm)	9.3 ± 1.7	9.3 ± 1.5	9.3 ± 2.0	.982
Inferior wall (mm)	9.1 ± 1.7	9.2 ± 1.5	9.1 ± 2.0	.856
Lateral wall (mm)	9.5 ± 1.8	9.9 ± 1.9	9.0 ± 1.6	.069
Thin point (mm)	2.3 ± 0.8	2.3 ± 0.7	2.2 ± 0.9	.757
Apex (mm)	4.6 ± 0.7	4.7 ± 0.7	4.3 ± 0.7	.043
Thin point _{indexed}	0.24 ± 0.07	0.24 ± 0.06	0.24 ± 0.08	.983
Apex _{indexed}	0.49 ± 0.06	0.50 ± 0.06	0.48 ± 0.06	.127

Values given are mean ± standard deviation. RS, apex rest perfusion score

*P for comparison of RS < 2 vs RS ≥ 2

Table 3. Base-to-apex gradient

	Base	Apex	Gradient	P-value*
Wall thickness (mm)	9.0 ± 1.6	4.6 ± 0.7	0.51 ± 0.07	< .001
Summed uptake (%)	76.2 ± 4.9	58.6 ± 7.1	0.77 ± 0.08	< .001
End-diastolic uptake (%)	56.7 ± 4.8	43.0 ± 5.9	0.76 ± 0.07	< .001
End-systolic uptake (%)	73.9 ± 7.1	62.9 ± 9.2	0.85 ± 0.09	< .001
MBF (mL/g/min)	0.82 ± 0.29	0.68 ± 0.28	0.83 ± 0.11	< .001
k2 (1/min)	0.25 ± 0.12	0.29 ± 0.18	1.16 ± 0.43	.027

Values given are mean ± standard deviation

*P for comparison of apex and base using a paired *t*-test

thickness ($r = -0.159$, $P = .237$). Likewise, there was no correlation between apical tracer uptake and apical wall thickness ($r = -0.080$, $P = .553$), nor did rest MBF correlate with either parameter (thin point: $r = -0.203$, $P = .129$; apical wall thickness: $r = -0.211$, $P = .115$). Analysis of k2 washout yielded no significant correlation with either thin point thickness ($r = -0.168$, $P = .230$) or apical wall thickness ($r = -0.023$, $P = .872$). Lastly, indexed myocardial wall thicknesses did not correlate with apical tracer uptake (thin point_{indexed}: $r = -0.128$, $P = .343$; apex_{indexed}: $r = -0.015$, $P = .914$), MBF (thin point_{indexed}: $r = -0.065$, $P = .630$; apex_{indexed}: $r = 0.130$, $P = .334$), or k2 washout (thin point_{indexed}: $r = -0.169$, $P = .226$; apex_{indexed}: $r = 0.062$, $P = .658$). Similarly, we found no correlation between the wall thickness gradient and summed uptake gradient ($r = -0.037$, $P = .783$), ED gradient ($r = 0.016$, $P = .906$), ES gradient ($r = 0.140$, $P = .299$), MBF gradient ($r = 0.036$, $P = .791$), or k2 gradient ($r = -0.021$, $P = .883$).

DISCUSSION

This is the first study to investigate the prevalence of apical thinning in PET-MPI and its possible association with true anatomical thinning of the left ventricular apical myocardium. In conjunction with partial volume effects, the latter has been suggested as a potential cause for apical thinning in SPECT-MPI. While this theory may be applicable in the setting of the lower spatial resolution in case of SPECT-MPI, only limited data exists for PET-MPI.²⁴

Both autopsy and CT-based studies have reported a high prevalence of focal reduction in myocardial wall thickness at the left ventricular apex. Bradfield et al. measured a thin point of < 2 mm in 97% of post-mortem hearts and in 67% of cases minimal thickness values were even lower than 1 mm, resulting in a mean apical thin point of 1.3 ± 0.7 mm.¹⁴ CT measurements

in patients without a history of cardiac disease confirmed these findings: Ferencik et al. reported a mean thin point of 1.7 ± 0.7 mm in vertical long axis reconstructions,¹⁶ and Johnson et al. measured 1.2 ± 1.1 mm.¹⁷ Using prospective ECG triggering and latest-generation CT technology with image acquisition at mid-diastole (i.e., at 75% of the R-R-interval), we observed slightly higher thin point thickness values (2.3 ± 0.8 mm).

In our study population, apical thinning in PET-MPI was very frequent with 93% of the patients having a normalized semiquantitative radiotracer uptake of < 70% at the apex despite the fact that we carefully excluded any patients with myocardial disease involving the apex. Automated scoring based on our historical normal database, which consequentially exhibits apical thinning as well, correctly classified only little more than half (54.4%) of the patients as having normal or only mildly reduced apical rest perfusion, rendering distinction between apical thinning and true apical scars for the interpreting physician difficult in clinical routine. The latter also strongly emphasizes the need for a continuous update of the normal database to match the acquisition protocols and processing algorithms in order to serve as a tool to reliably unmask apical thinning as an artifact. However, future studies directly comparing patients with true apical disease vs normal patients (preferably identified through anatomical imaging such as CCTA) may be needed to assess the true value of semi-automated scoring systems and potentially even recognize specific cut-off values for the apical region.

While we found a statistically significant difference in apical wall thickness in patients with $RS < 2$ as compared to patients with $RS \geq 2$, and while this difference may be considered negligibly small in absolute numbers (i.e., 0.4 mm), it has to be taken into account that the difference of observed tracer activity assessed by PET between two objects of varying size is influenced by differing recovery coefficients for these

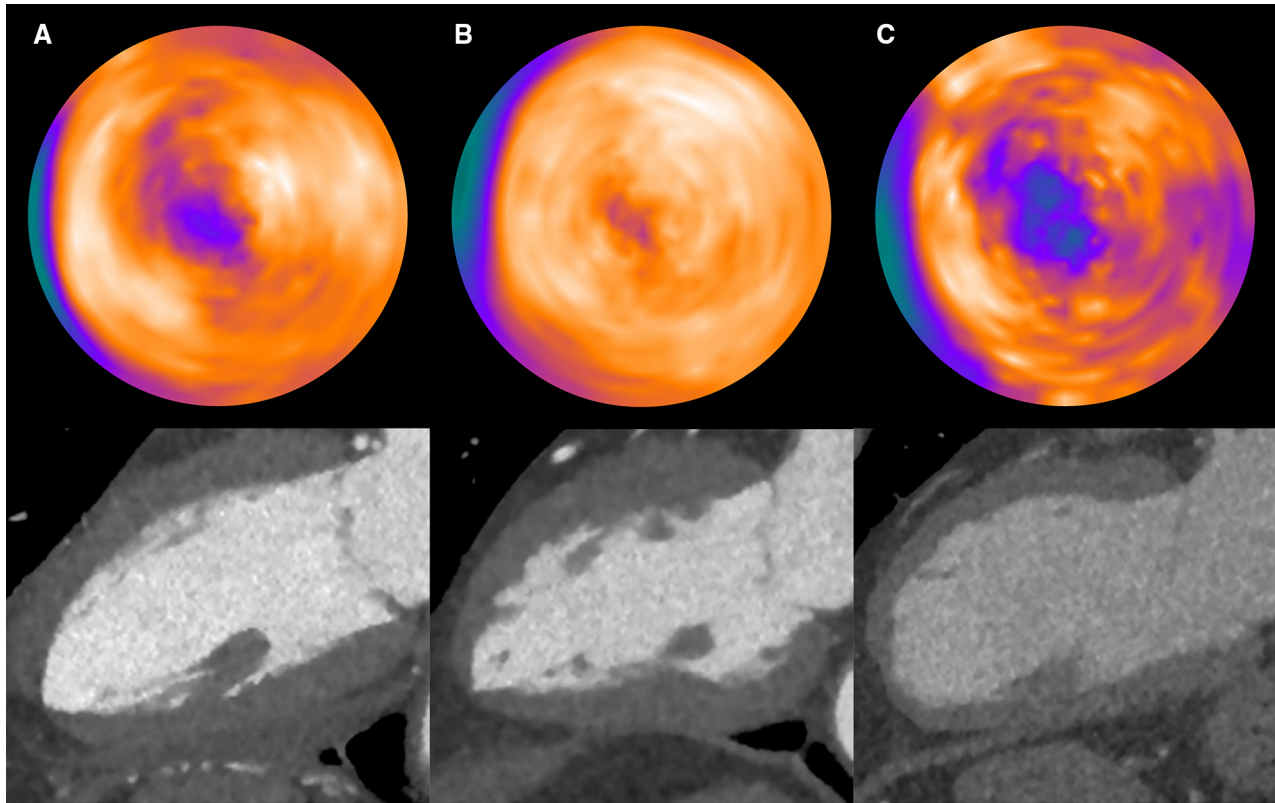


Figure 5. (A) Polar map display of semiquantitative tracer uptake (top) and vertical long axis view (bottom) of a patient exhibiting both visual apical thinning and true anatomical thinning (thin point thickness 1.4 mm). (B) example of anatomical thinning (thin point 1.4 mm) but only minimal visual apical thinning on PET-MPI. (C) occurrence of apical thinning in a patient without true anatomical thinning (thin point thickness 4.1 mm).

objects during image reconstruction. In our setting, however, we assume this relative change in observed tracer activity for a change in wall thickness of 0.4 mm to lie in the range of up to 3% which does not entirely explain the observed differences in semiquantitative normalized apical tracer uptake between both patient groups (i.e., $62.5 \pm 6.3\%$ vs $53.9 \pm 4.8\%$). By contrast, our findings suggest that the partial volume effect may play a more important role in the creation of the apical thinning phenomenon as a comparison of ED and ES datasets revealed a significant increase in apical tracer uptake and a less pronounced base-to-apex gradient at ES. However, limiting the analysis to ES did not eliminate apical thinning in the majority of patients as 74% still exhibited apical tracer uptake below the threshold of 70% (compared to 100% of patients on ED images). Interestingly, however, base-to-apex gradients were much less pronounced for the PET-derived parameters as compared to myocardial wall thickness, contrary to what would be expected from a very strong influence of the partial volume effect. Finally, apical myocardial wall

thickness did not correlate with tracer uptake in absolute numbers nor when comparing their respective base-to-apex gradients on summed, ED or ES images. From this, we conclude that other factors than true anatomical wall thickness and/or the partial volume effect play a more prominent role in the creation of the apical thinning artifact. This conclusion is corroborated by the fact that in some cases, apical thinning and severe reduction in apical myocardial wall thickness coincide (Figure 5A), while in others such an association cannot be found (Figure 5B). Finally, in some cases marked apical thinning can even be observed in patients with a thin point thickness of up to 4 mm (Figure 5C).

Apical thinning has been reported to be more pronounced on attenuation-corrected SPECT images than on non-corrected images (NC), with some authors suspecting an artifact induced by misalignment of the attenuation map,^{8,11} and with others assuming an unmasking of true anatomical wall thinning by AC.^{25–30} Specifically, it has been postulated that, on NC images, the apex shows falsely high counts as it is

located close to the chest wall and therefore less affected by tissue attenuation. AC algorithms for SPECT usually incorporate additional scatter compensation and resolution recovery which may further accentuate apical thinning.^{2,25,28} In light of this, it may be perceived as a limitation that we did not assess NC images in our study and therefore cannot rule out AC as a confounder. However, in PET-MPI, AC is a mandatory process according to current guidelines.¹ Additionally, all AC maps in the current study were manually checked for any perceivable misregistration and, while artifactual decreases in uptake because of AC misregistration are a proven concept, they are mostly encountered in the lateral and anterior wall rather than at the apex.^{8–10,31–33} Therefore, we would expect to see additional defects in other areas of the heart if AC was a major contributing factor to apical thinning. The same reasoning may also apply to respiratory and patient motion artifacts.²⁷ Regional differences in metabolic trapping of ¹³N-ammonia at the apex, as previously described in the inferior and posterolateral wall⁷, are not supported by our findings. While washout at the apex was higher compared to the base (Figure 4), it was subject to a high level of variation and did not differ between patients with mild or pronounced apical thinning.

Limitations

It may be perceived as a limitation that we used CT acquired at mid- to end-diastole (i.e., at 75% of the R–R interval) to assess anatomical wall thickness as this may not accurately reflect the true end-diastolic myocardial wall thickness. However, while such potential overestimation of the apical wall thickness may have had an impact on our analyses based on absolute measurements, the effect on the gradient analyses, which are based on ratios, should be negligible. Furthermore, the fact that some datasets were acquired and reconstructed differently, may be seen as a limitation namely because of the resulting differences in spatial resolution. Hence, we have performed all statistical analyses separately for both groups of patients as well and did not find any discrepant results that would have changed our conclusions. Finally, the historical normal database used in the present study, which comprises patients with low likelihood of CAD imaged during different scanner eras with differing acquisition protocols (e.g., 2D and 3D acquisition) may be imperfect and normal databases from other institutions may yield differing results.

NEW KNOWLEDGE GAINED

Apical thinning in ¹³N-ammonia PET-MPI has a very high prevalence.

Apical thinning as seen in PET-MPI is not solely attributable to true anatomical apical wall thickness and/or the partial volume effect.

CONCLUSION

Apical thinning is a highly prevalent finding during ¹³N-ammonia PET-MPI that is not solely attributable to true anatomical apical wall thickness or the partial volume effect. Other factors that yet need to be identified seem to have a more prominent impact.

Disclosure

The authors do not have any personal conflicts of interest to declare. However, the University Hospital Zurich holds a research contract with GE Healthcare.

References

1. Dilsizian V, Bacharach SL, Beanlands RS, Bergmann SR, Delbeke D, Dorbala S, et al. ASNC imaging guidelines/SNMMI procedure standard for positron emission tomography (PET) nuclear cardiology procedures. *J Nucl Cardiol.* 2016;23:1187–226.
2. Dvorak RA, Brown RKJ, Corbett JR. Interpretation of SPECT/CT myocardial perfusion images: Common artifacts and quality control techniques. *Radiographics.* 2011;31:2041–57.
3. Apostolopoulos DJ, Savvopoulos C. What is the benefit of CT-based attenuation correction in myocardial perfusion SPET? *Hell J Nucl Med.* 2016;19:89–92.
4. Case JA, Bateman TM. Taking the perfect nuclear image: Quality control, acquisition, and processing techniques for cardiac SPECT, PET, and hybrid imaging. *J Nucl Cardiol.* 2013;20:891–907.
5. Purser NJ, Armstrong IS, Williams HA, Tonge CM, Lawson RS. Apical thinning: Real or artefact? *Nucl Med Commun.* 2008;29:382–9.
6. Ficaro EP, Fessler JA, Shreve PD, Kritzman JN, Rose PA, Corbett JR. Simultaneous transmission/emission myocardial perfusion tomography. Diagnostic accuracy of attenuation-corrected ^{99m}Tc-sestamibi single-photon emission computed tomography. *Circulation.* 1996;93:463–73.
7. Beanlands RS, Muzik O, Hutchins GD, Wolfe ERJR, Schwaiger M. Heterogeneity of regional nitrogen 13-labeled ammonia tracer distribution in the normal human heart: Comparison with rubidium 82 and copper 62-labeled PTSM. *J Nucl Cardiol.* 1994;1:225–35.
8. Fricke H, Fricke E, Weise R, Kammeier A, Lindner O, Burchert W. A method to remove artifacts in attenuation-corrected myocardial perfusion SPECT Introduced by misalignment between emission scan and CT-derived attenuation maps. *J Nucl Med.* 2004;45:1619–25.

9. Gould KL, Pan T, Loghin C, Johnson NP, Guha A, Sdringola S. Frequent diagnostic errors in cardiac PET/CT due to misregistration of CT attenuation and emission PET images: A definitive analysis of causes, consequences, and corrections. *J Nucl Med.* 2007;48:1112–21.
10. Rajaram M, Tahari AK, Lee AH, Lodge MA, Tsui B, Nekolla S, et al. Cardiac PET/CT misregistration causes significant changes in estimated myocardial blood flow. *J Nucl Med.* 2013;54:50–4.
11. Slomka PJ, Diaz-Zamudio M, Dey D, Motwani M, Brodov Y, Choi D, et al. Automatic registration of misaligned CT attenuation correction maps in Rb-82 PET/CT improves detection of angiographically significant coronary artery disease. *J Nucl Cardiol.* 2015;22:1285–95.
12. Takamura T, Horiguchi Y, Kanna M, Matsushita H, Sudo Y, Kikuchi S, et al. Validation of prone myocardial perfusion SPECT with a variable-focus collimator versus supine myocardial perfusion SPECT with or without computed tomography-derived attenuation correction. *Ann Nucl Med.* 2015;29:890–6.
13. Tomiyama T, Ishihara K, Suda M, Kanaya K, Sakurai M, Takahashi N, et al. Impact of time-of-flight on qualitative and quantitative analyses of myocardial perfusion PET studies using (13)N-ammonia. *J Nucl Cardiol.* 2015;22:998–1007.
14. Bradfield JW, Beck G, Vecht RJ. Left ventricular apical thin point. *Heart.* 1977;39:806–9.
15. Cook DJ, Bailey I, Strauss HW, Rouleau J, Wagner HJ, Pitt B. Thallium-201 for myocardial imaging: Appearance of the normal heart. *J Nucl Med.* 1976;17:583–9.
16. Ferencik M, Abbara S, Hoffmann U, Cury RC, Brady TJ, Achenbach S. Left ventricular thin-point detection using multi-detector spiral computed tomography. *Am J Cardiol.* 2004;93:949–51.
17. Johnson KM, Johnson HE, Dowe DA. Left ventricular apical thinning as normal anatomy. *J Comput Assist Tomogr.* 2009;33:334–7.
18. Verberne HJ, Acampa W, Anagnostopoulos C, Ballinger J, Bengel F, Bondt P de, et al. EANM procedural guidelines for radionuclide myocardial perfusion imaging with SPECT and SPECT/CT: 2015 revision. *Eur J Nucl Med Mol Imaging* 2015;42:1929–40. http://eanm.org/publications/guidelines/2015_07_EANM_FINAL_myocardial_perfusion_guideline.pdf.
19. Slomka P, Nishina H, Berman D, Akincioglu C, Abidov A, Friedman J, et al. Automated quantification of myocardial perfusion SPECT using simplified normal limits. *J Nucl Cardiol.* 2005;12:66–77.
20. Gould KL, Nakagawa Y, Nakagawa K, Sdringola S, Hess MJ, Haynie M, et al. Frequency and clinical implications of fluid dynamically significant diffuse coronary artery disease manifest as graded, longitudinal, base-to-apex myocardial perfusion abnormalities by noninvasive positron emission tomography. *Circulation.* 2000;101:1931–9.
21. Valenta I, Quercioli A, Schindler TH. Diagnostic value of PET-measured longitudinal flow gradient for the identification of coronary artery disease. *JACC Cardiovasc Imaging.* 2014;7:387–96.
22. Hernandez-Pampaloni M, Keng FY, Kudo T, Sayre JS, Schelbert HR. Abnormal longitudinal, base-to-apex myocardial perfusion gradient by quantitative blood flow measurements in patients with coronary risk factors. *Circulation.* 2001;104:527–32.
23. Schindler TH, Facta AD, Prior JO, Campisi R, Inubushi M, Kreissl MC, et al. PET-measured heterogeneity in longitudinal myocardial blood flow in response to sympathetic and pharmacologic stress as a non-invasive probe of epicardial vasomotor dysfunction. *Eur J Nucl Med Mol Imaging.* 2006;33:1140–9.
24. Bartlett ML, Bacharach SL, Voipio-Pulkki LM, Dilsizian V. Artifactual inhomogeneities in myocardial PET and SPECT scans in normal subjects. *J Nucl Med.* 1995;36:188–95.
25. Pretorius PH, Narayanan MV, Dahlberg ST, Leppo JA, King MA. The influence of attenuation and scatter compensation on the apparent distribution of Tc-99m sestamibi in cardiac slices. *J Nucl Cardiol.* 2001;8:356–64.
26. Pretorius PH, King MA, Tsui BM, LaCroix KJ, Xia W. A mathematical model of motion of the heart for use in generating source and attenuation maps for simulating emission imaging. *Med Phys.* 1999;26:2323–32.
27. Pretorius PH, King MA. A study of possible causes of artifactual decreases in the left ventricular apex with SPECT cardiac perfusion imaging. *IEEE Trans Nucl Sci.* 1999;46:1016–23.
28. Links JM, Becker LC, Anstett F. Clinical significance of apical thinning after attenuation correction. *J Nucl Cardiol.* 2004;11:26–31.
29. Okuda K, Nakajima K, Matsuo S, Kondo C, Sarai M, Horiguchi Y, et al. Creation and characterization of normal myocardial perfusion imaging databases using the IQ SPECT system. *J Nucl Cardiol.* 2017. <https://doi.org/10.1007/s12350-016-0770-2>.
30. Okuda K, Nakajima K, Matsuo S, Wakabayashi H, Taki J, Kinuya S. Cause of apical thinning on attenuation-corrected myocardial perfusion SPECT. *Nucl Med Commun.* 2011;32:1033–9.
31. Tomita Y, Ishida M, Ichikawa Y, Suzawa N, Kobayashi S, Maeda H, et al. The effect of misregistration between CT-attenuation and PET-emission images in (13)N-ammonia myocardial PET/CT. *J Nucl Med Technol.* 2016;44:73–7.
32. Klingensmith WC, Noonan C, Goldberg JH, Buchwald D, Kimball JT, Manson SM. Decreased perfusion in the lateral wall of the left ventricle in PET/CT studies with (13)N-ammonia: Evaluation in healthy adults. *J Nucl Med Technol.* 2009;37:215–9.
33. Goetze S, Brown TL, Lavelly WC, Zhang Z, Bengel FM. Attenuation correction in myocardial perfusion SPECT/CT: Effects of misregistration and value of reregistration. *J Nucl Med.* 2007;48:1090–5.